3066–3077 Nucleic Acids Research, 2012, Vol. 40, No. 7 Published online 13 December 2011
doi:10.1093/nar/gkr1215

PfAlbas constitute a new eukaryotic DNA/RNA-binding protein family in malaria parasites

Arnaud Chêne[1,2], Shruthi S. Vembar[1,2], Loïc Rivière[1,2], José Juan Lopez-Rubio[1,2], Aurelie Claes[1,2], T. Nicolai Siegel[1,2], Hiroshi Sakamoto[1,2], Christine Scheidig-Benatar[1,2], Rosaura Hernandez-Rivas[3] and Artur Scherf[1,2,*]

[1]Institut Pasteur, Unité de Biologie des Interactions Hôte-Parasite, [2]CNRS, URA 2581, F-75015 Paris, France and [3]Departamento de Biomedicina Molecular, Centro de Investigación y de Estudios Avanzados del Instituto Politécnico Nacional (IPN), 07360, México D. F., México

Received April 7, 2011; Revised November 17, 2011; Accepted November 21, 2011

ABSTRACT

In *Plasmodium falciparum,* perinuclear subtelomeric chromatin conveys monoallelic expression of virulence genes. However, proteins that directly bind to chromosome ends are poorly described. Here we identify a novel DNA/RNA-binding protein family that bears homology to the archaeal protein Alba (Acetylation lowers binding affinity). We isolated three of the four PfAlba paralogs as part of a molecular complex that is associated with the *P. falciparum*-specific TARE6 (Telomere-Associated Repetitive Elements 6) subtelomeric region and showed in electromobility shift assays (EMSAs) that the PfAlbas bind to TARE6 repeats. In early blood stages, the PfAlba proteins were enriched at the nuclear periphery and partially co-localized with PfSir2, a TARE6-associated histone deacetylase linked to the process of antigenic variation. The nuclear location changed at the onset of parasite proliferation (trophozoite-schizont), where the PfAlba proteins were also detectable in the cytoplasm in a punctate pattern. Using single-stranded RNA (ssRNA) probes in EMSAs, we found that PfAlbas bind to ssRNA, albeit with different binding preferences. We demonstrate for the first time in eukaryotes that Alba-like proteins bind to both DNA and RNA and that their intracellular location is developmentally regulated. Discovery of the PfAlbas may provide a link between the previously described subtelomeric non-coding RNA and the regulation of antigenic variation.

INTRODUCTION

The apicomplexan parasite *Plasmodium falciparum*, the causative agent of the most lethal form of human malaria, undergoes a complex life cycle with distinct developmental stages both in the *Anopheles* mosquito and in the human hosts (1). To differentiate and adapt to an ever-changing environment the parasite applies different levels of regulation to modulate gene expression throughout its life cycle [reviewed in (2)]. Comparative genomic studies have revealed an apparent paucity of transcription factors (TFs) in apicomplexan proteomes although the basal set of TFs associated with RNA polymerase II are conserved (3–5). Nevertheless, the recent identification of the TF PfMyb1 in *P. falciparum* (6) and the DNA-binding protein family Apicomplexan Apetala2 (ApiAP2) (7–10), strongly suggests that apicomplexan parasites possess a larger repertoire of elements regulating gene expression than previously thought. Detailed transcriptome analyses have also revealed that the plasmodial intra-erythrocytic developmental cycle is accompanied by a continuous cascade of gene transcription (11,12). However, increasing evidence supports the idea that various degrees of post-transcriptional control exist in many, if not all, growth stages (13,14). One such mechanism, translational repression, post-transcriptionally regulates a subset of mRNAs during gametocyte-to-ookinete transition in *P. berghei* (15), and proteins that are involved in this process are also conserved in *P. falciparum*.

Epigenetic regulation in *P. falciparum* was first demonstrated for multicopy genes involved in antigenic variation implicating histone marks (acetylation) and the histone deacetylase PfSir2 in variegated gene expression at chromosome ends (16,17). Subsequent genome-wide analyses using ChIP-on-chip revealed a general role for

*To whom correspondence should be addressed. Tel: +33 1 45 68 86 16; Fax: +33 145 68 83 48; Email: artur.scherf@pasteur.fr

The authors wish it to be known that, in their opinion, the first two authors should be regarded as joint First Authors.

several histone marks (methylation and acetylation) in *P. falciparum* gene regulation (18,19). Moreover, non-coding highly repetitive subtelomeric DNA elements called TAREs (Telomere-Associated Repetitive Elements) present virtually at all *P. falciparum* chromosome ends play a central role in virulence gene regulation. The TAREs recruit to the nuclear periphery several epigenetic factors that are involved in the silencing of major virulence gene families (17,19–21). We termed the TARE-associated protein complex Perinuclear Epigenetic Repression Center (PERC) (19). TARE6, which is the largest repetitive region, is composed of 21-bp repetitive units stretching over 6 to 23 kb on different chromosome ends. TARE6 plays a central role in the clustering of telomeres at the nuclear periphery (22,23). Specific proteins that directly bind to TARE6 DNA remain elusive.

In this work, we purified the TARE6-associated protein complex and identified a new DNA/RNA-binding protein family in *P. falciparum* composed of four paralogs. All members contain a domain presenting strong homology to the archaeal chromatin protein family Alba (Acetylation lowers binding affinity; InterPro IPR002775). We show that the *P. falciparum* Alba proteins (PfAlba1-4) are able to directly bind to TARE6 DNA repeats and to single-stranded RNA (ssRNA) with different sequence specificities. These proteins are highly enriched at the nuclear periphery in ring stages and expand to the cytoplasm in more mature stages where they form speckles. Our results demonstrate for the first time in a eukaryotic system that Alba-like proteins bind to both DNA and RNA suggesting a dual role in chromatin biology and RNA regulation.

MATERIAL AND METHODS

Parasite culture

Plasmodium falciparum blood stage parasites were cultivated as previously described (24).

Nuclear and cytoplasmic extracts

Nuclear and cytoplasmic extracts were prepared as previously described (17) with some modifications. A total of 5×10^9 parasites were isolated from infected erythrocytes by saponine lysis, resuspended in 1 ml of lysis buffer (10 mM HEPES pH 7.9, 10 mM KCl, 0.1 mM EDTA, 0.1 mM EGTA, 1 mM DTT, 0.65% NP-40) supplemented with protease inhibitors (Complete, Roche) and incubated for 30 min at 4°C. Total parasite lysis was achieved by 200 strokes in a prechilled Dounce homogenizer. The lysate was centrifuged for 10 min at 14 000 rpm at 4°C. The supernatant representing the cytoplasmic fraction was recovered, aliquoted and stored at −80°C. The nuclei pellet was washed three times with phosphate-buffered saline (PBS) and then resuspended in 100 µl of extraction buffer (20 mM HEPES pH 7.9, 400 mM NaCl, 1 mM EDTA, 1 mM EGTA, 1 mM DTT) supplemented with protease inhibitors and incubated with vigorous shaking for 30 min at 4°C. The preparation was then centrifuged for 10 min at 14 000 rpm at 4°C. The supernatant representing the nuclear fraction was recovered, aliquoted and stored at −80°C. The purity of the extracts was checked by western blotting, probing the membrane with anti-HSP70 and anti-$H3_{me3K9}$ antibodies.

Identification of TARE6-associated proteins

Electromobility shift assays (EMSAs) using a radiolabeled TARE6 DNA probe (Supplementary Table S1) and ring stage nuclear extracts were performed as previously described (17). The DNA–protein complex was analyzed on a non-denaturing polyacrylamide gel, the complex was cut out of the gel and proteins were recovered by electro-elution in running buffer (0.025 M Tris, 0.192 M glycine, 1% SDS) using an Electro-Eluter (Model 422; Bio-Rad) at 10 mA for 5 h. After elution, the proteins were dialyzed, lyophilized and resuspended in PBS. The proteins were quantified by Lowry's method, resolved by SDS–PAGE and visualized by silver staining using the Silver–Quest Staining Kit (Invitrogen). The identity of the proteins was established by mass spectrometry

Biotinylated TARE6 DNA was immobilized onto Streptavidin-coupled Dynabeads following an incubation in binding buffer (20 mM HEPES pH 7.9, 100 mM KCl, 2 mM $MgCl_2$, 0.5 mM EDTA, 1 mM DTT, 0.4 mM $ZnSO_4$, 40 mM $ZnCl_2$, 10% Glycerol and 0.1% Triton X-100) for 1 h at 4°C. The biotinylated 165-bp KAHRP DNA probe was obtained by PCR amplification with primers KAHRPups and KAHRP2 (Supplementary Table S1) and immobilized onto Streptavidin-coupled Dynabeads as described above. DNA-coated beads were collected, washed twice in binding buffer and incubated with nuclear extracts for 30 min at 25°C. Protein–bead complexes were washed four times with binding buffer containing 250 mM NaCl and proteins were eluted with Laemmli sample buffer without any dye by boiling at 95°C for 5 min. Then, the proteins were concentrated and desalted using Amicon Centricon columns and analyzed by SDS–PAGE followed by silver staining. Finally, the proteins associated with TARE6 and KAHRP DNA were identified by mass spectrometry.

Mass spectrometry

The in-gel digestion of proteins was carried out according to the manufacturer's manual (Pierce, Rockford, IL). The desired band was excised, destained and possible disulfide bonds reduced with tris (2-carboxyethyl) phosphine (TCEP) and alkylated with iodoacetamide. Then, the gel pieces were dehydrated with acetonitrile and rehydrated with 100 ng trypsin (Promega, Madison, WI) in 25 mM ammonium bicarbonate solution and were incubated at 37°C overnight. The tryptic fragments were extracted from the gel by adding 1% trifluroacetic acid. Next, the peptides were purified with a C18 reversed-phase minicolumn filled into a micropipette tip, i.e. ZipTip C18 (Millipore, Bedford, MA). Purified peptides were cocrystallized with a-cyano-4-hydroxy cinnamic acid matrix (Applied Biosystems, Foster City, CA, USA) on a matrix-assisted laser desorption ionization (MALDI) target plate. Both mass spectrometry (MS) and MS/MS spectra were acquired in a MALDI–time of flight

(MALDI–TOF/TOF) Mass Spectrometer (Applied Biosystems 4800 Proteomics Analyzer) in the reflector mode. Calibration was updated before each acquisition using a standard peptide mixture according to the instrument's protocol. Protein identification was performed using the GPS Explorer software (Applied Biosystems) with the MASCOT search engine (Matrix Science). The search was performed against the NCBInr 20080502 database (6493741 sequences; 2216039219 residues) and the Mascot significance threshold was set at $P = 0.05$. Individual Ions scores >33 indicated identity or extensive homology and were considered to be significant.

Antibodies (Abs)

Rabbit polyclonal Abs against PfAlba1-4 resulting from immunizations of rabbits with PfAlba-specific synthetic peptides were purchased from GenScript Corporation (genscript.com). The peptide sequences are listed in Supplementary Table S2. Mouse polyclonal Abs against PfAlba1-4 were isolated from the sera of six mice immunized with recombinant GST-tagged PfAlba proteins. Briefly, each recombinant protein was emulsified with complete adjuvant (Sigma) and 100 µg was inoculated into a single mouse. Following the inoculation series, animals were sacrificed and serum was collected. Immunoglobulins were purified from the serum by protein A-sepharose chromatography following standard procedures (Pharmacia).

Recombinant proteins

The coding region of PfAlba1-4 and the two tandem AP2 domains of PfSip2 (PFF0200c; residues 177–312) were PCR-amplified from cDNA prepared from 3D7 parasites and cloned into the pGEX-3X vector (GE Healthcare), downstream of the gene encoding GST. Penta-His tagged PfAlba3 was obtained by cloning the PF10_0063 gene into the pET28a vector (Novagen). The primer pairs used are displayed in Supplementary Table S3. Recombinant protein expression was carried out in BL21-CodonPlus(DE3)-RIL *Escherichia coli* cells (Stratagene). The recombinant proteins were induced with 0.1 mM IPTG at an OD_{600} of 0.6 for 3 h at 37°C. GST-fusion proteins were purified using Glutathione Sepharose 4B beads (GE Healthcare) and His-tagged proteins were purified using a Ni-NTA Superflow gravity column (Qiagen) according to manufacturer instructions. The resulting eluates were resolved using SDS–PAGE and protein purity was determined by Coomassie blue staining.

DNA and RNA EMSAs

The 79-bp biotinylated TARE6 probe was obtained as previously described (21). The 79-bp biotinylated AP2 probe containing two GTGCA motifs was obtained by PCR amplification of the 5′ regulatory region of the MAL7P1.119 gene from genomic DNA isolated from 3D7 parasites. The primers used are displayed in Supplementary Table S3. Fragments of dsDNA were obtained by hybridization of the sense oligonucleotide with its complementary anti-sense sequence. All other unlabeled and biotin-labeled oligonucleotides (Supplementary Table S1) were purchased from Eurogentec. EMSAs were performed as previously described (17).

ssRNA oligonucleotides (Supplementary Table S1) were labeled at the 5′-end with [γ^{32}-P]-ATP using the Ready-To-Go T4 Polynucleotide Kinase kit (Amersham Biosciences). Radiolabeled oligonucleotides were separated from free [γ^{32}-P]-ATP using Sephadex G-25 columns (Roche). RNA EMSAs were performed as previously described (25).

Immunofluorescence microscopy

Synchronized cultures of the 3D7 *P. falciparum* parasite line were washed in PBS, lysed in saponine (0.015%) and fixed in suspension with 4% paraformaldehyde (Electron Microscopy Sciences) for 15 min at room temperature (RT). Fixed parasites were blocked for 30 min with PBS+1% bovine serum albumin (BSA) and incubated with the primary Abs diluted in PBS+1% BSA for 45 min at RT. After washing with PBS, parasites were incubated with the secondary Abs diluted in PBS+1%BSA for 30 min at RT. Finally, labeled parasites were deposited on microscope slides and mounted in Vectashield anti-fading solution supplemented with DAPI (Vector Laboratories). Images were captured using a Nikon Eclipse 80i optical microscope and analyzed with the NIS-Elements BR software (Nikon). For confocal microscopy, images were captured using a Nikon Eclipse TE2000-E confocal microscope and analyzed with the EZ-C1 software (Nikon).

Western blotting

Parasite cytoplasmic and nuclear extracts (equivalent to 5×10^7 parasites per lane) were resolved on a 4–12% SDS–PAGE gel, transferred onto a nitrocellulose membrane and subject to western blotting with specific Abs against the PfAlbas (Supplementary Table S2), anti-$H3_{Me3K9}$ (Abcam) and anti-HSP70 (26). After incubation with secondary antibodies (horseradish-conjugated), membranes were developed with Super-Signal West Pico Chemiluminescent Substrate (Pierce).

Electron microscopy

Ultrathin sections of *P. falciparum* blood stage parasites were immuno-stained for electron microscopy (EM) analysis. *Plasmodium falciparum*-infected erythrocytes were fixed in 1% glutaraldehyde in RPMI-HEPES buffer for 1 h at 4°C. After washing, polymerization in Agar type IX and dehydratation with ethanol, the samples was transferred in LR-White (London Resin Compagny Ltd, Berkshire, UK) and polymerized for 12 h at 4°C. Ultrathin sections were collected and mounted on Cu/Pd grids. Sections were blocked in PBS containing 5% (wt/vol) nonfat dried milk and 0.01% (wt/vol) Tween-80 followed by a washing with PBS containing 0.8% BSA (fraction V) and 0.01% Tween-80. The washed grids were incubated for 2.5 h with anti-PfAlba Abs diluted in the above-mentioned solution. Samples were washed and incubated for 25 min with 10 nm

protein A-colloidal gold (Cell Microscopy Center, University Medical Center Utrech, The Netherlands). Washed sections were stained for 15 min with aqueous 4% uranyl acetate followed by a staining of 2 min with 1% lead citrate. For double labeling, the first labeling was performed with anti-Histone 3 Abs (Abcam ab1791) diluted at 1/100 and revealed with 15 nm protein A-colloidal gold. The grids were washed and fixed with 1% glutaraldehyde in PBS for 5 min and blocked. After washing, the second labeling was performed with anti-PfAlba Abs diluted at 1/50 and revealed with 10 nm protein A-colloidal gold according to the same protocol. The grids were washed and stained with aqueous 4% uranyl acetate followed by a staining of 2 min with 1% lead citrate. Sections were analyzed with a JEOL JEM-1200EX electron microscope.

PfAlba-Ty1 transfectant parasites

The PfAlba1-Ty1C and PfAlba4-Ty1C constructs were obtained by replacing the pfenr-GFP sequence contained in the pLN-ENR-GFP plasmid (27) with the coding regions of PF08_0074 and MAL13P1.237 respectively. In addition, a nucleotide sequence encoding for two repeats of the Ty1 epitope (LEVHTNQDPLD) was inserted downstream of the PfAlba genes. Episomal transfection of 3D7 parasites was performed as previously described (28). PfAlba-Ty1 expression was detected using a rabbit anti-Ty1 Ab (Genscript) or the mouse BB2 monoclonal anti-Ty1 Ab (29).

Analytical ultracentrifugation

His-tagged PfAlba3 samples in PBS (8 μM) were centrifuged at a speed of 42 000 rpm in a Beckman Coulter XL-I analytical ultracentrifuge at 20°C using a AN60-Ti rotor equipped with 12 mm double-sector epon centrepieces. Detection of the protein concentration as a function of radial position and time was performed by optical density measurements at a wavelength of 220 nm. The following parameters were calculated using Sednterp 1.09 and used for the analysis of the experiment: partial specific volume $\bar{\upsilon} = 0.735$ ml/g, viscosity $\eta = 1.052$ cP and density $\rho = 1.019$ g/ml. Sedimentation velocity data analysis was performed by continuous size distribution analysis c(s) using the program Sedfit 12.0 (30) (available at http://www.analyticalultracentrifugation.com). All the c(s) distributions were calculated with a fitted frictional ratio f/f_0 and a maximum entropy regularization procedure with a confidence level of 0.95.

RESULTS

The TARE6-associated complex contains proteins that are homologous to the archaeal chromatin protein family Alba

Plasmodium falciparum chromosome ends are composed of degenerate G-rich heptameric repeats, the telomeres, followed by a mosaic of six non-coding subtelomeric regions, TARE1-6 (Figure 1A) (31,32). To define the molecular nature of the protein complex associated with TARE6 (17), we used two different experimental approaches (EMSA and oligonucleotide pull down), each using a labeled TARE6 probe containing three repetitive units (Supplementary Table S1). In the first approach (Figure 1B), the protein complex that bound to radiolabeled TARE6 in EMSAs was isolated from ring stage parasite nuclear extracts using gel electrophoresis and subjected to mass spectrometry. In the second approach (Figure 1B), biotinylated TARE6 was immobilized onto streptavidin-coated beads and proteins from ring stage parasite nuclear extracts that bound to TARE6 were identified by mass spectrometry. A similar pull down experiment was performed using a probe from the promoter region of the Knob-Associated Histidine-Rich (KAHRP) gene (PFB0100c) as a non-TARE DNA control.

LC–MS/MS analysis revealed that TARE6 interacts with a large molecular complex of over 30 proteins (Supplementary Table S4); only five of these proteins, including a few histones, were identified in the pull down experiment performed using the KAHRP probe (Supplementary Table S4). Intriguingly, three members of the TARE6-associated complex PF08_0074, MAL13P1.233 and MAL13P1.237 (plasmodb.org) (Figure 1C) presented homology to the archaeal DNA/RNA-binding protein family Alba, that plays an important role in chromatin organization in archaea (33). Further sequence analysis of the *P. falciparum* genome revealed the existence of a fourth paralog, PF10_0063. We name the four members of the newly described Alba-like protein family in *P. falciparum* as PfAlba1, PfAlba2, PfAlba4 and PfAlba3, respectively. Assessment of protein architecture using the Pfam (www.ebi.ac.uk/pfam) and InterPro (www.ebi.ac.uk/interpro) databases (Figure 1D) showed that PfAlba1 (27 kDa) and PfAlba2 (25 kDa), in addition to their N-terminal Alba-like domains (residues 8–123 and residues 9–87 respectively), contain multiple C-terminal RGG-box (arginine- and glycine-rich) RNA-binding domains. PfAlba3 (12 KDa), the shortest member of the PfAlba protein family is essentially composed of one module of the Alba-like domain (residues 10–102). Finally, PfAlba4, a 42 kDa protein, is composed of two distinct domains: an N-terminal Alba-like domain (residues 19–115) and a central membrane-tethering ENTH/VHS domain (residues 175–229) (InterPro ID: IPR008942). Multiple sequence alignment analysis showed that the PfAlbas possess conserved orthologs in other Plasmodial species (Supplementary Figure S1).

To conclusively establish the presence of the PfAlbas in the TARE6-associated protein complex, we performed EMSAs with the radiolabeled TARE6 probe, nuclear extracts of ring stage parasites and purified rabbit antibodies raised against PfAlba1, PfAlba2, PfAlba3 or PfAlba4 (Supplementary Table S2). The anti-PfAlba1, -PfAlba2 and -PfAlba4 antibodies 'super-shifted' the TARE6-associated protein complex in a dose-dependent manner (Figure 1E; complex 'SC') whereas no super-shift was observed using antibodies directed against PfAlba3 (data not shown). Pre-immune sera did not lead to super-shifts. Taken together, we show that the TARE6-associated molecular complex contains three

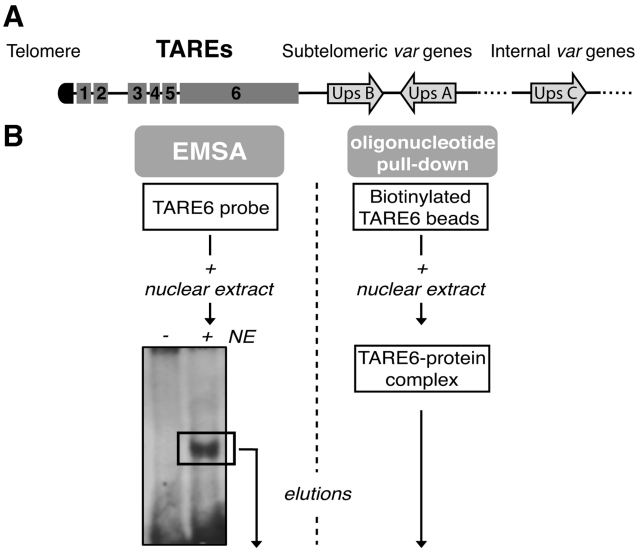

C

Mass spectrometry analysis

	EMSA		Oligonucleotide pull-down	
Protein ID PlasmoDB	Unique Peptide	Mascot Score	Unique Peptide	Mascot Score
MAL13P1.237	11	383	3	209
PF08_0074	0	-	4	131
MAL13P1.233	0	-	1	49

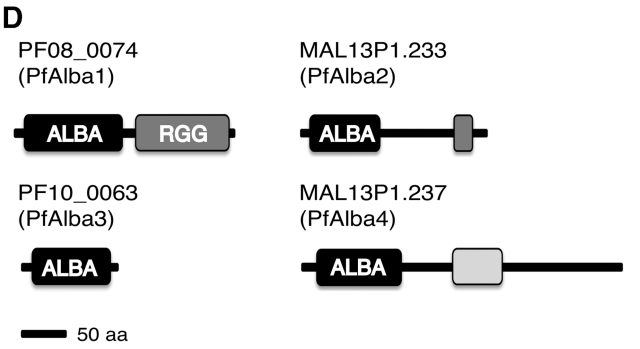

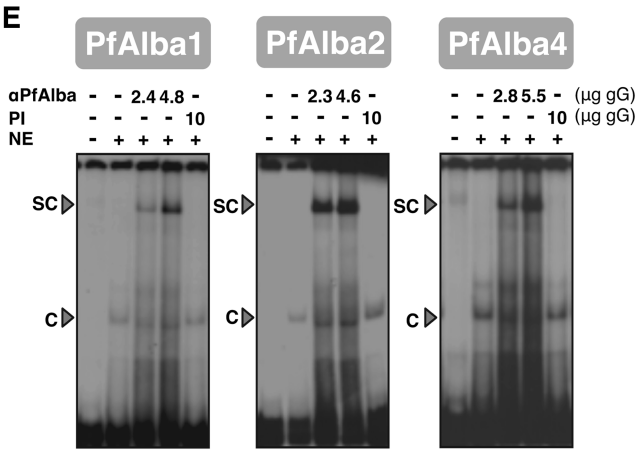

Figure 1. TARE6 associates with a large molecular complex containing paralogs of the PfAlba protein family. (**A**) Schematic representation of the subtelomeric regions of *P. falciparum* chromosomes. The non-coding TAREs are adjacent to the subtelomeric *var* genes. paralogs of a previously uncharacterized protein family in *P. falciparum,* PfAlba1, PfAlba2 and PfAlba4, bearing homology to the archaeal chromatin protein family Alba.

PfAlbas bind to DNA with relaxed sequence specificity

In archaea, Alba proteins bind to DNA and are proposed to play an important role in chromatin architecture (33). To elucidate whether the PfAlbas are capable of binding to DNA and directly interacting with TARE6, we performed EMSAs using recombinant GST-tagged PfAlbas (Supplementary Figure S2) and a biotinylated version of the double-stranded TARE6 DNA probe described above. Parasite nuclear extract served as a positive control for TARE6 binding. As shown in Figure 2A, all four PfAlbas were able to bind to the TARE6 probe in a dose-dependent manner. In particular, with increasing concentrations of PfAlba3, the DNA–protein complex migrated at a slower rate suggesting that this PfAlba, which contains just an Alba domain, could form higher order complexes similar to its archaeal counterparts (34). Our data demonstrate for the first time in a eukaryotic system that Alba-like proteins can directly bind to DNA.

In archaea, Albas have been reported to bind to DNA without sequence specificity (35). First focusing on PfAlba4, we wanted to assess if the same holds true for the *P. falciparum* Albas. Therefore, we designed a biotinylated DNA probe containing two tandem GTG CA motifs that represent the recognition sequence of PfSIP2, a recently described *P. falciparum* DNA-binding protein of the ApiAP2 family (8,9). This probe is of similar length to the TARE6 probe (79 bp) and is referred to as AP2 throughout this study (Supplementary Table S1). As expected, recombinant GST-tagged PfSIP2 bound to the AP2 probe and inversely did not bind to the TARE6 probe, which lacks GTGCA motifs (left panel of Figure 2B). Next, incubation of PfAlba4 with the AP2 probe did not lead to any detectable band shift, although under the same conditions, PfAlba4 bound to the TARE6 probe (left panel of Figure 2B). These data suggest that, in contrast to the archaeal Albas, PfAlba4 may bind to DNA with an apparent sequence preference. To test this further, we assessed if

Figure 1. Continued
(**B**) Flowchart representation of the two approaches used to isolate the protein complex that associates with TARE6 *in vitro*. (**C**) Out of over 30 protein candidates identified by mass spectrometry (Supplementary Table S4), three proteins showed similarity to the archaeal DNA/RNA-binding protein family Alba. Plasmodb accession numbers and the number of unique peptides identified are tabulated. (**D**) Pfam and InterPro databases were used to determine the architecture of PfAlba proteins. The Alba-like domain is depicted in black, the ENTV/VHS domain in light gray and the RGG-box RNA-binding domain in dark gray. The scale bar represents 50 amino acids. (**E**) To assess the presence of PfAlba1, PfAlba2 and Pfalba4 in the molecular complex associated with TARE6, a ^{32}P-labeled TARE6 probe was incubated with *P. falciparum* ring stage nuclear extract 'NE' and subject to EMSAs. A single DNA–protein complex 'C' formed when the TARE6 probe was incubated with nuclear extract alone. Addition of increasing amounts of specific antibodies (μg of Immunoglobulin G indicated as μg gG) against PfAlba4 (Ab 237–1), PfAlba1 (Ab 74–2) or PfAlba2 (Ab 233) led to the formation of a super-shift complex 'SC'. Incubation with the respective pre-immune sera 'PI' did not result in a super-shift.

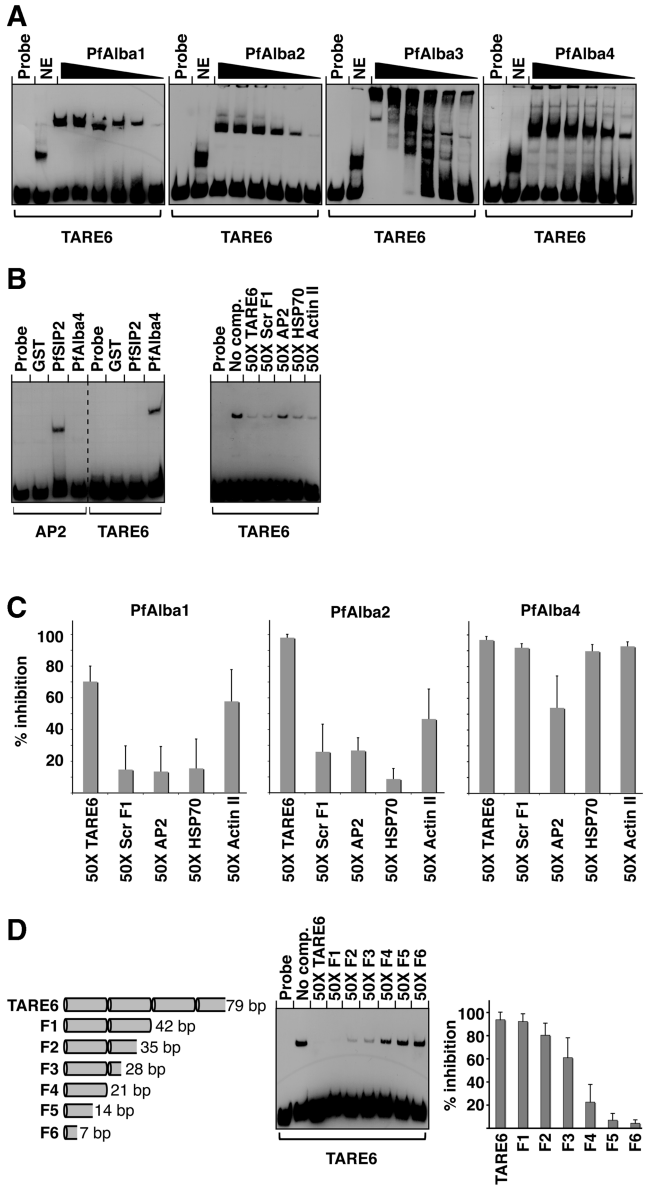

Figure 2. PfAlbas bind to DNA with relaxed sequence specificity. (**A**) In order to assess the DNA-binding properties of PfAlbas, a biotin-labeled TARE6 probe was incubated with *P. falciparum* nuclear extract 'NE' or increasing concentrations [ranging from 0.5 to 5 μM] of recombinant PfAlba1-4 and subjected to EMSAs. (**B**) Left panel: To assess PfAlba4 specificity, biotin-labeled TARE6 and AP2 probes were each incubated with either 5 μM GST or 0.1 μM PfSIP2 or 0.5 μM PfAlba4; Right panel: Competition EMSAs were also used to determine the binding specificity of PfAlba4 to DNA. 0.5 μM recombinant PfAlba4 was incubated with biotin-labeled TARE6 (0.28 nM) in the absence (No comp.) or presence of 50-fold excess of the indicated unlabeled dsDNA competitor. (**C**) Quantification of competition EMSAs performed using PfAlba1, PfAlba2 and PfAlba4, and the indicated competitor probes. The percentage inhibition was calculated by normalizing each datapoint to TARE6–PfAlba binding in the absence of competitor. Error bars represent the standard deviation of data obtained from three independent experiments. (**D**) Fragments of TARE6 DNA ranging from 7 to 42 bp in length (left panel) were used in competition EMSAs to determine the minimal length required by PfAlba4 for DNA binding. Data were quantified as described in the legend of Figure 2C. Error bars represent the standard deviation of data obtained from three independent experiments.

a number of non-TARE6 DNA sequences would be able to compete for binding of PfAlba4 to TARE6 in EMSAs. In addition to an unlabeled AP2 probe, we designed two probes from the coding regions of PfHSP70 (PF08_0054) and PfActin-II (PF14_0124) and one probe containing a scrambled nucleotide sequence from the first 42 bp of the TARE6 probe (Scr F1; Supplementary Table S1). All competition experiments used a 50-fold excess of the unlabeled 'competitor' probe. Surprisingly, the ScrF1, HSP70 and Actin-II probes were almost as potent in inhibiting TARE6–PfAlba4 binding as the unlabeled TARE6 probe (97% inhibition) (right panel of Figure 2B and C). In contrast, the unlabeled AP2 probe was less efficient at inhibition (54%), supporting the poor AP2–PfAlba4 binding observed in Figure 2B (left panel). Taken together, our results demonstrate that recombinant PfAlba4 binds to DNA with relaxed sequence preference. To determine if other PfAlbas exhibit similar sequence requirements, we performed TARE6–PfAlba1 or –PfAlba2-binding EMSAs with the competitor probes described above. We observed that the non-TARE6 probes were less efficient at inhibiting TARE6–PfAlba1/2 binding (Figure 2C) as compared to TARE6–PfAlba4 binding. Interestingly, a 50-fold excess of the unlabeled TARE6 probe inhibited TARE6–PfAlba1 binding up to just 70%. This suggests that the PfAlbas present differential sequence preferences *in vitro* with PfAlba1 possessing the highest affinity for TARE6.

Finally, to define the minimum length required by PfAlba4 for DNA binding, we performed competition EMSAs using TARE6 fragments of varying sizes (42–7 bp) (Figure 2D). Two repetitive units, i.e. the 42 bp probe, were able to fully inhibit TARE6–PfAlba4 binding whereas the percent inhibition by shorter TARE6 fragments gradually decreased, with a sharp drop at 14 bp. Our results define a minimal DNA length for efficient PfAlba4 recruitment to be >14 bp. This could also explain our inability to identify specific DNA-binding motifs for PfAlba1 and PfAlba4 in protein-binding microarrays that used 10 bp oligomers (M. Llinás and T. Campbell, personal communication).

PfAlbas localize to perinuclear foci in ring stages and expand to the cytoplasm in mature forms

Our *in vitro* data identified the PfAlbas as novel DNA-binding proteins with potential multiple targets in the nucleus. Next, we investigated the cellular localization of these proteins during *P. falciparum* blood stages. We performed immunofluorescence assays on synchronized ring, trophozoite and schizont parasite cultures using either affinity-purified antibodies raised in rabbits against synthetic peptides of PfAlba1-4 or polyclonal antibodies obtained from mice immunized with recombinant GST-tagged PfAlba1-4 (Supplementary Table S2). Antibodies against PfAlba1, PfAlba2 and PfAlba4 stained the nuclear periphery in a spotted pattern similar to that observed for telomere clusters (Figure 3A and Supplementary Figure S3) (21); the antibodies against PfAlba3 did not give a signal under the conditions tested. Moreover, co-localization assays with antibodies

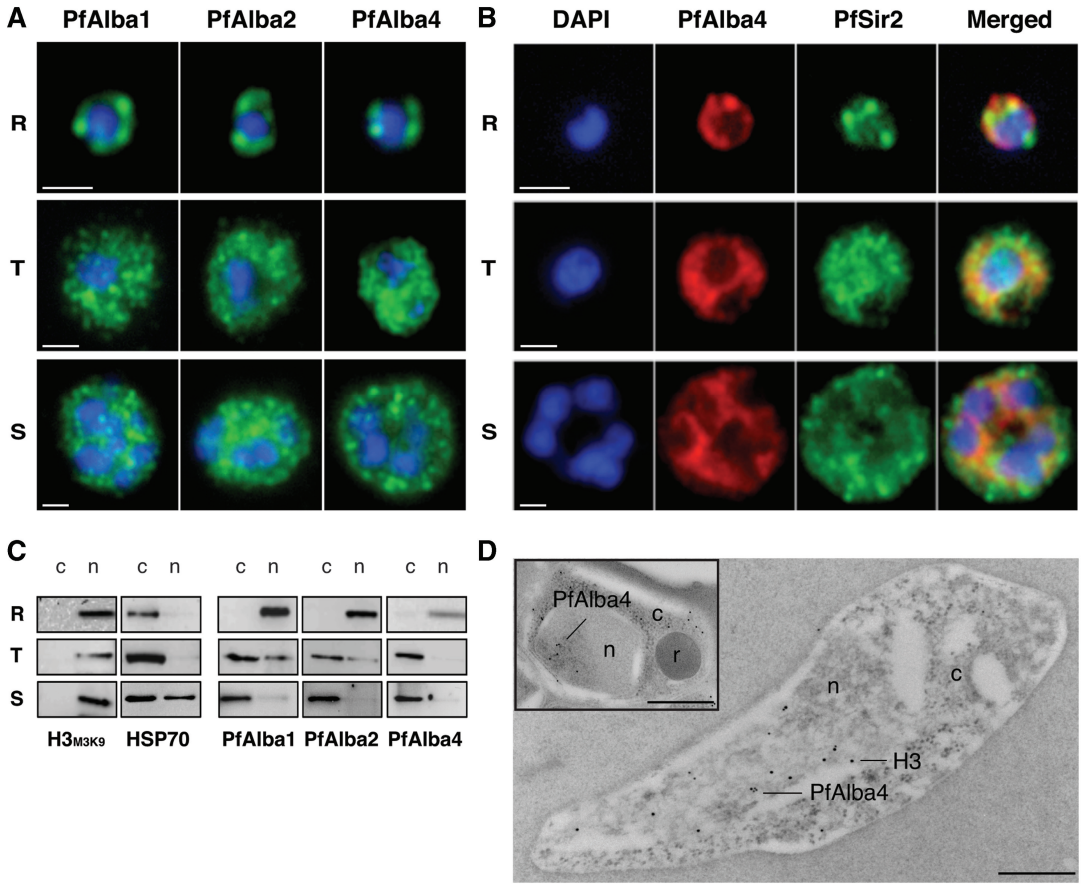

Figure 3. PfAlbas localize to perinuclear foci in ring stages and expand to the cytoplasm in mature forms. (**A**) Immunofluorescence analysis of PfAlba1, PfAlba2 and Pfalba4 distribution throughout the parasite life cycle (Rings, Trophozoites, Schizonts). The anti-PfAlba antibodies (Ab 74–2 for PfAlba1; Ab 233 for PfAlba2; Ab 237–2 for PfAlba4) were used at 5.5, 4.5 and 8 μg/ml, respectively. Anti-rabbit Alexa-488 secondary antibodies (Molecular Probes) were used at a dilution of 1:500. Scale bars represent 1 μm. (**B**) Immunofluorescence analysis of 3D7 Rings, Trophozoites and Schizonts stained with anti-PfAlba4 (red) and anti-PfSir2 (green) antibodies. Scale bar represents 1 μm. (**C**) Western blot analysis of nuclear and cytoplasmic fractions obtained from synchronous cultures of Ring, Trophozoite and Schizont parasites. The equivalent of 5×10^7 parasites was loaded in each lane and probed with the indicated anti-PfAlba antibody (Ab 74–2 for PfAlba1; Ab 233 for PfAlba2; Ab 237–1 for PfAlba4). Anti-$H3_{M3K9}$ (nuclear marker) and anti-HSP70 antibodies were used to determine fractionation efficiency. (**D**) Immuno-EM was performed on ring stage parasites using anti-PfAlba4 antibodies (Ab 237–2) bound to 10 nm gold particles and anti-H3 antibodies bound to 15 nM gold particles. The inset shows a single developing merozoite within schizont-stage parasites labeled with anti-PfAlba4 antibodies (Ab 237–2) bound to 10 nm gold particles; n = nucleus, c = cytoplasm, r = rhoptry; Scale bars represent 500 nm.

against PfSir2 and PfAlba4 indicated that the nuclear distribution of PfAlba4 partially overlaps with an epigenetic factor belonging to the TARE6-associated PERC (Figure 3B). In contrast, during the trophozoite and schizont stages, a strong signal was detected for PfAlba1, PfAlba2 and PfAlba4 in the cytoplasm, primarily in a punctate manner (Figure 3A and Supplementary Figure S3A). This distribution is reminiscent of m-RNA containing P-granules observed in *P. berghei* gametocytes (36). Also, co-localization assays with anti-PfSir2 and -PfAlba4 antibodies showed that the PfAlba4 signal dissociates from the PfSir2 signal in mature stages (Figure 3B), especially when analyzed by confocal microscopy (Supplementary Figure S3B).

Western blot analysis of the cytoplasmic and nuclear fractions reflected the dynamic changes in the subcellular compartmentalization of PfAlba1, PfAlba2 and PfAlba4 during the parasite life cycle (Figure 3C). These PfAlbas were detected exclusively in the nuclear fraction in the ring stage whereas in mature stages, cytoplasmic localization became more dominant. Protein relocation can often be imputed to either proteolytic processing or sumoylation events. Because the PfAlbas migrate at their predicted size during gel electrophoresis and western blotting, we suppose that other modifications that could modulate the function of the PfAlbas without drastically changing the protein size may control their subcellular localization. Again, the anti-PfAlba3 antibodies did not detect a band at the predicted size in western blotting although they cross-reacted with recombinant GST–PfAlba3 under the same conditions (data not shown).

In order to further define the exact localization of the PfAlbas within the nucleus, we immunolabeled ultrathin sections of blood stage parasites using antibodies directed against the PfAlbas and performed EM. We present here images obtained for PfAlba4 (Figure 3D). In the ring stage, we detected PfAlba4 uniquely in the nucleus. Since the nuclear membrane is difficult to visualize in

immuno-EM in the ring stage, co-labeling with antibodies directed against histone H3 was used to determine the area of the nucleus in this parasite form. The images localize PfAlba4 at the nuclear periphery. This pattern was confirmed in developing merozoites (inset of Figure 3D) where we could detect distinct clusters of PfAlba4 at the periphery of the nuclei. This pattern was similar to the one previously observed for PfSir2 (17). Although western blots indicated that most of the PfAlba4 is in the cytoplasmic fraction of schizonts (Figure 3C), our EM finding can be explained by a better accessibility of PfAlba4 in the nucleus to antibodies under the EM fixation conditions as compared to the cytoplasm. Similar experiments performed with anti-PfAlba1 are depicted in Supplementary Figure S3C. In all sets of experiments, incubation with pre-immune sera did not give any signal. Our data demonstrate that the PfAlbas occupy distinct cellular compartments hinting at multiple distinct roles during the asexual blood stage.

PfAlbas bind to RNA with differential specificities

Their cytoplasmic location raises the question as to whether the PfAlbas play a role in the RNA biology of *P. falciparum* blood stages. To investigate this, we asked whether the PfAlbas could bind to RNA by performing EMSAs with recombinant GST-tagged PfAlbas and 22-mer ssRNA oligonucleotides, polyA and polyU (Supplementary Table S1). Because of the AT-richness of the *P. falciparum* genome [~75% in exons (31)], these ssRNAs are the most representative of native transcripts. Parasite nuclear extracts and the ApiAP2 DNA-binding protein PfSip2 were used as controls. We observed that all four Albas could bind to polyA and polyU, albeit with different specificities (Figure 4A). At the protein concentrations tested, PfAlba1 showed a 2-fold stronger affinity for polyA as compared to polyU while PfAlba2 and PfAlba4 bound to both probes at similar levels. Finally, PfAlba3, which contains just the Alba-like domain, exhibited a high affinity for polyA and a lower affinity for polyU. These data suggest that the PfAlbas may bind to different RNA targets *in vivo*. Interestingly, for PfAlba2–4, multiple species of ssRNA–protein complexes were observed, hinting at protein oligomerization.

We next wanted to assess if the ssRNA oligonucleotides polyA and polyU could compete for the binding of PfAlbas to TARE6 DNA. Continuing to focus on PfAlba4, we performed TARE6 EMSAs using a 50-fold excess of polyA and polyU as compared to the biotinylated TARE6 probe. PolyA abolished TARE6–PfAlba4 binding to the same extent as a 50-fold excess of unlabeled TARE6 whereas polyU had only a minor effect on the binding of PfAlba4 to TARE6 (Figure 4B). That RNA molecules compete for PfAlba4 DNA binding strongly suggests that PfAlba1 utilizes the same domain to bind to DNA and RNA. This is an intriguing concept with potential regulatory implications in the nucleus.

PfAlba3 forms an elongated dimer

The PfAlba3–DNA and –RNA complexes migrate at different sizes with an increase in protein concentration

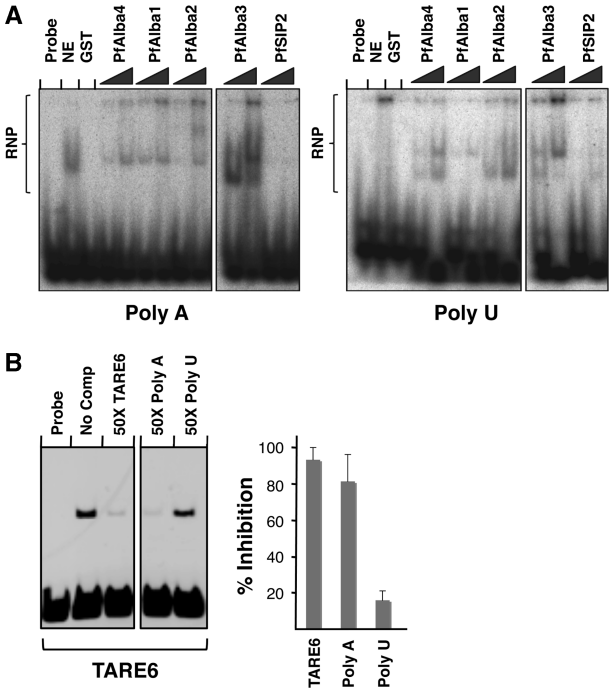

Figure 4. PfAlbas bind to ssRNA *in vitro*. (**A**) To determine binding to the radiolabeled ssRNA probes polyA (left panel) and polyU (right panel), RNA EMSAs were performed in the absence (Probe alone) or presence of nuclear extracts from *P. falciparum* trophozoites (NE), 1.5 µg GST, or two concentrations (0.3 and 1.2 µg) of the indicated GST-tagged PfAlba protein. A GST-tagged version of the DNA-binding domain of PfSip2 served as the negative control. RNP = Ribonucleoprotein complex. (**B**) The ability of the ssRNA probes to compete for PfAlba4-TARE6 binding was assessed by using 50-fold molar excess of the indicated unlabeled probes in TARE6 DNA EMSAs. Controls included reactions either lacking PfAlba4 (Probe alone) or containing 50-fold molar excess of unlabeled TARE6. Data were quantified as described in the legend of Figure 2*C*. Error bars represent the standard deviation of data obtained from three independent experiments.

(Figures 2A and 4A). Given that the archaeal Albas bind to DNA by forming dimers and dimer–dimer stacks (34), we wanted to determine the oligomeric status of recombinant PfAlba3. Because GST alone exists as a dimer (37), results obtained from GST–PfAlba3 native gel electrophoresis and size exclusion chromatography analyses were inconclusive (data not shown). Instead, we generated penta-His-tagged PfAlba3 by affinity purification, enriched it by size-exclusion chromatography (Figure 5A) and subjected it to analytical ultracentrifugation (Figure 5B). At a concentration of 8 µM, the data revealed the presence of a single species with a sedimentation coefficient of 1.3 ± 0.2 S and a frictional ratio of 2.1, indicating that His-PfAlba3 is an elongated dimer in solution.

DISCUSSION

Our work provides the first description of homologs of the archaeal histone-like protein family Alba as DNA and RNA-binding proteins in a eukaryotic system. After the identification of the gene encoding for the founding Alba

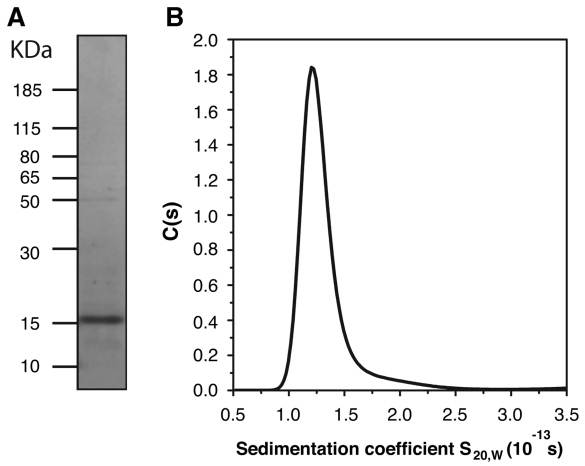

Figure 5. PfAlba3 exists as an elongated dimer in solution. (**A**) Amido black staining of purified penta-His-tagged PfAlba3 subjected to SDS–PAGE and transferred to a nitrocellulose membrane. (**B**) Analytical ultracentrifugation followed by sedimentation coefficient (S20,w) distribution analysis [c(s)] of His-PfAlba3. Data were collected under standard conditions (i.e. in water at 20°C) at a protein concentration of 8 μM.

family member (38), Sac10b, homologs have been found in all archaeal species. Archaeal Alba homologs have been shown to bind to DNA without sequence specificity (35) and to RNA *in vitro* and *in vivo* (39). Our novel findings in *P. falciparum* highlight the evolutionary conservation as well as diversity of the eukaryotic Alba proteins. First, similar to their archaeal homologs, the PfAlbas bind to DNA and RNA (Figures 2 and 4). Second, the cellular distributions of the PfAlbas are developmentally regulated resulting in different subcellular localizations during the 48-h blood stage cycle (Figures 3 and Supplementary Figure S3). Notably, the PfAlba4 nuclear staining during ring stages (i.e. foci in the nuclear periphery) partially follows the same pattern as the subtelomere-associated histone deacetylase PfSir2 (17). Given that the affinity of archaeal Albas for DNA is increased by Sir2-mediated deacetylation (40), by analogy, deacetylation of the PfAlbas by PfSir2 may increase their DNA-binding affinity within the restricted nuclear compartment and specifically enrich these proteins at subtelomeric regions of *P. falciparum* chromosomes. Third, in three of the four PfAlba members, the Alba domain has been fused either to an RGG-box domain or to an ENTH/VHS domain (Figure 1D). This adds a potential regulatory element to the Alba domain that may recruit other molecules to the PfAlba DNA and/or RNA-binding sites.

In spite of PfAlba3's absence in the TARE6-associated complex (Figure 1), our EMSA results show that all members of the PfAlba protein family have the capacity to bind to a TARE6 DNA probe *in vitro* (Figure 2A). Because PfAlba3 is composed of a single domain, the Alba domain (Figure 1D), DNA recognition by all PfAlba family members is in all likelihood attributable to their Alba domains, with the other domains determining specificity. This is further supported by the molecular models of the tertiary structure of the Alba domains from PfAlba1–4 constructed using the archaeal Alba Sso10b (PDB ID: 1h0x) as a template (Supplementary Figure S4). These models show that the structures of the PfAlba1–4 Alba domains are likely to be conserved including the extended β-hairpin that is proposed to interact with DNA in archaea (35). Interestingly, the lysine residue that is deacetylated by archaeal Sir2 is conserved in PfAlba2 and 4 (Supplementary Figure S4).

Archaeal Alba binds to DNA as a dimer that spans ~15 bp of dsDNA with the two β-hairpins formed by each Alba monomer presumably interacting with equivalent minor grooves (35). Sequence alignments of Alba domains from several organisms including *P. falciparum* have revealed that the residues mapping to the dimer interface are well-conserved implying a conserved dimeric quaternary structure (41). Because PfAlba3 is an elongated dimer in solution (Figure 5B), it is reasonable to assume that the mechanism by which the PfAlbas bind to DNA is similar to the one in archaea and requires protein dimerization. This is also in line with our results indicating that dsDNA fragments <15 bp are poor competitors of TARE6–PfAlba4 binding (Figure 2D). Furthermore, it has been reported that the affinity of Alba proteins for DNA is increased by hetero-dimerization and dimer–dimer stacking interactions (34,42). Given that PfAlba2 and PfAlba4 interacted reciprocally in a genome-wide *P. falciparum* yeast-two hybrid screen (43), PfAlba heterodimer formation possibly occurs *in vivo* influencing DNA/RNA affinity and/or sequence specificity. Finally, in archaea, Albas bind to DNA without sequence specificity (35). Genome-wide analysis of Sso10b distribution by chromatin immunoprecipitation demonstrated that the protein was uniformly and ubiquitously distributed on the chromosome of *S. solfataricus* (35). Nevertheless, a recent study showed that an Alba homolog Mmm10b in the mesophile *Methanococcus maripaludis* binds to an 18-bp degenerate DNA motif with apparent sequence specificity (44). This indicates that the DNA specificity and functions of Alba homologs have greatly diverged amongst different organisms. To begin to study this, we transfected wild-type 3D7 parasites with Ty1 epitope-tagged versions of PfAlba1 and PfAlba4 (Supplementary Figure S5) and performed ChIP-seq analysis using anti-Ty1 antibodies. However, we were unable to obtain enrichment of the PfAlbas at specific genomic loci under the preliminary conditions tested (data not shown). That the tagged proteins localized to the same cellular compartments as their endogenous PfAlba counterparts (Supplementary Figure S5D) suggested that they were functional and provides additional support for a perinuclear role for the PfAlbas in ring stage parasites. Overall, we hypothesize that the PfAlbas contribute to the recruitment of epigenetic factors to the PERC, although other functions related to internal chromosomal regions that localize to the nuclear periphery cannot be ruled out.

As stated above, the differential cellular localization of the PfAlbas during distinct stages of the 48-h intra-erythrocytic parasite growth cycle may provide vital clues to the *in vivo* functions of these proteins. In rings,

PfAlba1, PfAlba2 and PfAlba4 localization is restricted to the nuclear periphery (Figures 3A and Supplementary Figure S3) and this is presumably required for chromatin regulation. Around 18 h post-invasion, i.e. in trophozoites, the majority of PfAlba1, PfAlba2 and PfAlba4 are found as cytoplasmic speckles (>50% based on western blot analysis in Figure 3C), which persists during schizogony. We therefore hypothesize that the PfAlbas perform RNA-dependent functions in the cytoplasm of blood stages. This is supported by our observation that the PfAlbas directly bind to ssRNA (Figure 4A). The only published example of Plasmodial Albas comes from the rodent malaria parasite *P. berghei*, where three Alba homologs co-purified with components of cytoplasmic P-granules from sexual stages, i.e. gametocytes (36). Although no direct PbAlba–RNA binding was shown, the authors proposed that the PbAlbas participate in the repression of certain stage-specific mRNA species. However, translational repression has not been demonstrated for *P. falciparum* asexual blood stages indicating that PfAlba–RNA interaction could modulate additional cellular processes in this parasite. TARE1-6 sequences do not exist in rodent malaria parasites and it will be interesting to explore if *P. berghei* Albas bind to DNA. Phylogenetic analysis categorized the Alba-like domains of the PfAlbas as belonging to the RPP20 (PfAlba3&4) and RPP25 (PfAlba1&2) RNase-P superfamilies (41), which are involved in the processing of t-RNAs and ribosomal RNAs by forming heterodimers (45), and suggested that the plasmodial Albas may preferentially bind to RNA. Such an interaction with RNA could stabilize specific RNA molecules or enable RNA secondary structure formation, in turn affecting PfAlba localization. An RNA 'chaperoning' role has previously been described for the Hfq protein in *E. coli* (46). Another possibility is that post-translational modifications such as acetylation, phospohorylation and/or methylation could modulate PfAlbas' affinity for DNA versus RNA in a stage-specific manner and trigger transport from the nucleus to the cytoplasm. This is not unprecedented because deacetylation of Sso10b by Sir2 has been shown to increase Sso10b's DNA-binding affinity (40) and phosphorylation and methylation of arginine residues in the RGG domain of yeast Npl3p have been shown to alter its nuclear import by affecting interaction with Mtr10p (47). Finally, RNA binding may also be an important determinant of PfAlbas' nuclear function. Recently, non-coding RNA (ncRNA) transcripts corresponding to TARE6 and the adjacent *var* intronic regions have been identified in *P. falciparum* (48,49). Given that the PfAlbas bind to RNA *in vitro* (Figure 4), these proteins may provide a direct link between the previously described subtelomeric non-coding RNA and the regulation of antigenic variation.

In conclusion, the characterization of the *P. falciparum* Albas reveals for the first time that Alba-like proteins are capable of DNA and RNA binding in a eukaryotic organism. Our data implicate a dual function for the PfAlbas in chromatin biology and in RNA regulation. Overall, this opens up new avenues to explore key aspects of not just the biology of chromosome ends such as the molecular mechanism of antigenic variation and the spatial organization of *P. falciparum* chromosomes into perinuclear foci, but also the biology of post-transcriptional gene regulation. Our inability to obtain PfAlba knockout parasites suggests that the PfAlbas are crucial for parasite survival. Inducible protein knockdown parasite lines for PfAlbas are now needed to unravel their physiological role during the various stages of the intra-erythrocytic cycle of *P. falciparum*.

SUPPLEMENTARY DATA

Supplementary Data are available at NAR online: Supplementary figures S1–S5 and Supplementary tables S1–S4.

ACKNOWLEDGEMENTS

The authors would like to thank M. Llinás and T. Campbell from Princeton University, Princeton, USA, for performing the Protein Binding Microarrays, Adéla Nacer for her help with confocal imaging, and Bertrand Raynal from the Plate-forme de Biophysique des Macromolecules et de leurs Interactions at Insitut Pasteur, Paris, for his help with the analytical centrifugation experiments.

FUNDING

European Research Council Executive Agency Advanced Grant (PlasmoEscape 250320); the Fondation de Recherche Médicale (DMI20091117322); the Network of Excellence EVIMALAR of the European Commission (FP7); and the Consejo Nacional de Ciencia y Tecnológia (45687/A-1 to R.H.R.); postdoctoral fellowship from the Conseil régional d'Île-de-France (DIM Malinf) to A.C. Funding for open access charge: European Research Council Executive Agency Advanced Grant (PlasmoEscape 250320).

Conflict of interest statement. None declared.

REFERENCES

1. Garnham,P.C. (1963) Distribution of simian malaria parasites in various hosts. *J. Parasitol.*, **49**, 905–911.
2. Llinas,M., Deitsch,K.W. and Voss,T.S. (2008) Plasmodium gene regulation: far more to factor in. *Trends Parasitol.*, **24**, 551–556.
3. Templeton,T.J., Iyer,L.M., Anantharaman,V., Enomoto,S., Abrahante,J.E., Subramanian,G.M., Hoffman,S.L., Abrahamsen,M.S. and Aravind,L. (2004) Comparative analysis of apicomplexa and genomic diversity in eukaryotes. *Genome Res.*, **14**, 1686–1695.
4. Callebaut,I., Prat,K., Meurice,E., Mornon,J.P. and Tomavo,S. (2005) Prediction of the general transcription factors associated with RNA polymerase II in Plasmodium falciparum: conserved features and differences relative to other eukaryotes. *BMC Genomics*, **6**, 100.
5. Coulson,R.M., Hall,N. and Ouzounis,C.A. (2004) Comparative genomics of transcriptional control in the human malaria parasite Plasmodium falciparum. *Genome Res.*, **14**, 1548–1554.
6. Boschet,C., Gissot,M., Briquet,S., Hamid,Z., Claudel-Renard,C. and Vaquero,C. (2004) Characterization of PfMyb1 transcription factor during erythrocytic development of 3D7 and F12

Plasmodium falciparum clones. *Mol. Biochem. Parasitol.*, **138**, 159–163.
7. Balaji,S., Babu,M.M., Iyer,L.M. and Aravind,L. (2005) Discovery of the principal specific transcription factors of Apicomplexa and their implication for the evolution of the AP2-integrase DNA binding domains. *Nucleic Acids Res.*, **33**, 3994–4006.
8. Flueck,C., Bartfai,R., Niederwieser,I., Witmer,K., Alako,B.T., Moes,S., Bozdech,Z., Jenoe,P., Stunnenberg,H.G. and Voss,T.S. (2010) A major role for the Plasmodium falciparum ApiAP2 protein PfSIP2 in chromosome end biology. *PLoS Pathog.*, **6**, e1000784.
9. De Silva,E.K., Gehrke,A.R., Olszewski,K., Leon,I., Chahal,J.S., Bulyk,M.L. and Llinas,M. (2008) Specific DNA-binding by apicomplexan AP2 transcription factors. *Proc. Natl Acad. Sci. USA*, **105**, 8393–8398.
10. Yuda,M., Iwanaga,S., Shigenobu,S., Mair,G.R., Janse,C.J., Waters,A.P., Kato,T. and Kaneko,I. (2009) Identification of a transcription factor in the mosquito-invasive stage of malaria parasites. *Mol. Microbiol.*, **71**, 1402–1414.
11. Bozdech,Z., Llinas,M., Pulliam,B.L., Wong,E.D., Zhu,J. and DeRisi,J.L. (2003) The transcriptome of the intraerythrocytic developmental cycle of Plasmodium falciparum. *PLoS Biol.*, **1**, E5.
12. Le Roch,K.G., Zhou,Y., Blair,P.L., Grainger,M., Moch,J.K., Haynes,J.D., De La Vega,P., Holder,A.A., Batalov,S., Carucci,D.J. *et al.* (2003) Discovery of gene function by expression profiling of the malaria parasite life cycle. *Science*, **301**, 1503–1508.
13. Sam-Yellowe,T.Y., Florens,L., Johnson,J.R., Wang,T., Drazba,J.A., Le Roch,K.G., Zhou,Y., Batalov,S., Carucci,D.J., Winzeler,E.A. *et al.* (2004) A Plasmodium gene family encoding Maurer's cleft membrane proteins: structural properties and expression profiling. *Genome Res.*, **14**, 1052–1059.
14. Foth,B.J., Zhang,N., Mok,S., Preiser,P.R. and Bozdech,Z. (2008) Quantitative protein expression profiling reveals extensive post-transcriptional regulation and post-translational modifications in schizont-stage malaria parasites. *Genome Biol.*, **9**, R177.
15. Mair,G.R., Braks,J.A., Garver,L.S., Wiegant,J.C., Hall,N., Dirks,R.W., Khan,S.M., Dimopoulos,G., Janse,C.J. and Waters,A.P. (2006) Regulation of sexual development of Plasmodium by translational repression. *Science*, **313**, 667–669.
16. Duraisingh,M.T., Voss,T.S., Marty,A.J., Duffy,M.F., Good,R.T., Thompson,J.K., Freitas-Junior,L.H., Scherf,A., Crabb,B.S. and Cowman,A.F. (2005) Heterochromatin silencing and locus repositioning linked to regulation of virulence genes in Plasmodium falciparum. *Cell*, **121**, 13–24.
17. Freitas-Junior,L.H., Hernandez-Rivas,R., Ralph,S.A., Montiel-Condado,D., Ruvalcaba-Salazar,O.K., Rojas-Meza,A.P., Mancio-Silva,L., Leal-Silvestre,R.J., Gontijo,A.M., Shorte,S. *et al.* (2005) Telomeric heterochromatin propagation and histone acetylation control mutually exclusive expression of antigenic variation genes in malaria parasites. *Cell*, **121**, 25–36.
18. Salcedo-Amaya,A.M., van Driel,M.A., Alako,B.T., Trelle,M.B., van den Elzen,A.M., Cohen,A.M., Janssen-Megens,E.M., van de Vegte-Bolmer,M., Selzer,R.R., Iniguez,A.L. *et al.* (2009) Dynamic histone H3 epigenome marking during the intraerythrocytic cycle of Plasmodium falciparum. *Proc. Natl Acad. Sci. USA*, **106**, 9655–9660.
19. Lopez-Rubio,J.J., Mancio-Silva,L. and Scherf,A. (2009) Genome-wide analysis of heterochromatin associates clonally variant gene regulation with perinuclear repressive centers in malaria parasites. *Cell Host Microbe*, **5**, 179–190.
20. Perez-Toledo,K., Rojas-Meza,A.P., Mancio-Silva,L., Hernandez-Cuevas,N.A., Delgadillo,D.M., Vargas,M., Martinez-Calvillo,S., Scherf,A. and Hernandez-Rivas,R. (2009) Plasmodium falciparum heterochromatin protein 1 binds to tri-methylated histone 3 lysine 9 and is linked to mutually exclusive expression of var genes. *Nucleic Acids Res.*, **37**, 2596–2606.
21. Mancio-Silva,L., Rojas-Meza,A.P., Vargas,M., Scherf,A. and Hernandez-Rivas,R. (2008) Differential association of Orc1 and Sir2 proteins to telomeric domains in Plasmodium falciparum. *J. Cell. Sci.*, **121**, 2046–2053.
22. O'Donnell,R.A., Freitas-Junior,L.H., Preiser,P.R., Williamson,D.H., Duraisingh,M., McElwain,T.F., Scherf,A., Cowman,A.F. and Crabb,B.S. (2002) A genetic screen for improved plasmid segregation reveals a role for Rep20 in the interaction of Plasmodium falciparum chromosomes. *EMBO J.*, **21**, 1231–1239.
23. Figueiredo,L.M., Freitas-Junior,L.H., Bottius,E., Olivo-Marin,J.C. and Scherf,A. (2002) A central role for Plasmodium falciparum subtelomeric regions in spatial positioning and telomere length regulation. *EMBO J.*, **21**, 815–824.
24. Nunes,M.C., Goldring,J.P., Doerig,C. and Scherf,A. (2007) A novel protein kinase family in Plasmodium falciparum is differentially transcribed and secreted to various cellular compartments of the host cell. *Mol. Microbiol.*, **63**, 391–403.
25. Hong,X., Zang,J., White,J., Wang,C., Pan,C.H., Zhao,R., Murphy,R.C., Dai,S., Henson,P., Kappler,J.W. *et al.* Interaction of JMJD6 with single-stranded RNA. *Proc. Natl Acad. Sci. USA*, **107**, 14568–14572.
26. Blisnick,T., Lema,F., Mazie,J.C. and Pereira da Silva,L.P. (1988) Plasmodium falciparum: analysis of B epitopes of a polypeptide antigen expressed in Escherichia coli, using monoclonal antibodies. *Exp. Parasitol.*, **67**, 247–256.
27. Nkrumah,L.J., Muhle,R.A., Moura,P.A., Ghosh,P., Hatfull,G.F., Jacobs,W.R. Jr and Fidock,D.A. (2006) Efficient site-specific integration in Plasmodium falciparum chromosomes mediated by mycobacteriophage Bxb1 integrase. *Nat. Methods*, **3**, 615–621.
28. Fidock,D.A. and Wellems,T.E. (1997) Transformation with human dihydrofolate reductase renders malaria parasites insensitive to WR99210 but does not affect the intrinsic activity of proguanil. *Proc. Natl Acad. Sci. USA*, **94**, 10931–10936.
29. Bastin,P., Bagherzadeh,Z., Matthews,K.R. and Gull,K. (1996) A novel epitope tag system to study protein targeting and organelle biogenesis in Trypanosoma brucei. *Mol. Biochem. Parasitol.*, **77**, 235–239.
30. Brown,P.H. and Schuck,P. (2006) Macromolecular size-and-shape distributions by sedimentation velocity analytical ultracentrifugation. *Biophys. J.*, **90**, 4651–4661.
31. Gardner,M.J., Hall,N., Fung,E., White,O., Berriman,M., Hyman,R.W., Carlton,J.M., Pain,A., Nelson,K.E., Bowman,S. *et al.* (2002) Genome sequence of the human malaria parasite Plasmodium falciparum. *Nature*, **419**, 498–511.
32. Figueiredo,L.M., Pirrit,L.A. and Scherf,A. (2000) Genomic organisation and chromatin structure of Plasmodium falciparum chromosome ends. *Mol. Biochem. Parasitol.*, **106**, 169–174.
33. Sandman,K. and Reeve,J.N. (2005) Archaeal chromatin proteins: different structures but common function? *Curr. Opin. Microbiol.*, **8**, 656–661.
34. Jelinska,C., Petrovic-Stojanovska,B., Ingledew,W.J. and White,M.F. (2010) Dimer-dimer stacking interactions are important for nucleic acid binding by the archaeal chromatin protein Alba. *Biochem. J.*, **427**, 49–55.
35. Wardleworth,B.N., Russell,R.J., Bell,S.D., Taylor,G.L. and White,M.F. (2002) Structure of Alba: an archaeal chromatin protein modulated by acetylation. *EMBO J.*, **21**, 4654–4662.
36. Mair,G.R., Lasonder,E., Garver,L.S., Franke-Fayard,B.M., Carret,C.K., Wiegant,J.C., Dirks,R.W., Dimopoulos,G., Janse,C.J. and Waters,A.P. (2010) Universal features of post-transcriptional gene regulation are critical for Plasmodium zygote development. *PLoS Pathog.*, **6**, e1000767.
37. Wilce,M.C. and Parker,M.W. (1994) Structure and function of glutathione S-transferases. *Biochim. Biophys. Acta*, **1205**, 1–18.
38. Forterre,P., Confalonieri,F. and Knapp,S. (1999) Identification of the gene encoding archeal-specific DNA-binding proteins of the Sac10b family. *Mol. Microbiol.*, **32**, 669–670.
39. Guo,R., Xue,H. and Huang,L. (2003) Ssh10b, a conserved thermophilic archaeal protein, binds RNA in vivo. *Mol. Microbiol.*, **50**, 1605–1615.
40. Bell,S.D., Botting,C.H., Wardleworth,B.N., Jackson,S.P. and White,M.F. (2002) The interaction of Alba, a conserved archaeal chromatin protein, with Sir2 and its regulation by acetylation. *Science*, **296**, 148–151.
41. Aravind,L., Iyer,L.M. and Anantharaman,V. (2003) The two faces of Alba: the evolutionary connection between proteins participating in chromatin structure and RNA metabolism. *Genome Biol.*, **4**, R64.

42. Jelinska,C., Conroy,M.J., Craven,C.J., Hounslow,A.M., Bullough,P.A., Waltho,J.P., Taylor,G.L. and White,M.F. (2005) Obligate heterodimerization of the archaeal Alba2 protein with Alba1 provides a mechanism for control of DNA packaging. *Structure*, **13**, 963–971.
43. LaCount,D.J., Vignali,M., Chettier,R., Phansalkar,A., Bell,R., Hesselberth,J.R., Schoenfeld,L.W., Ota,I., Sahasrabudhe,S., Kurschner,C. *et al.* (2005) A protein interaction network of the malaria parasite Plasmodium falciparum. *Nature*, **438**, 103–107.
44. Liu,Y., Guo,L., Guo,R., Wong,R.L., Hernandez,H., Hu,J., Chu,Y., Amster,I.J., Whitman,W.B. and Huang,L. (2009) The Sac10b homolog in Methanococcus maripaludis binds DNA at specific sites. *J. Bacteriol.*, **191**, 2315–2329.
45. Hands-Taylor,K.L., Martino,L., Tata,R., Babon,J.J., Bui,T.T., Drake,A.F., Beavil,R.L., Pruijn,G.J., Brown,P.R. and Conte,M.R. (2010) Heterodimerization of the human RNase P/MRP subunits Rpp20 and Rpp25 is a prerequisite for interaction with the P3 arm of RNase MRP RNA. *Nucleic Acids Res.*, **38**, 4052–4066.
46. Brennan,R.G. and Link,T.M. (2007) Hfq structure, function and ligand binding. *Curr. Opin. Microbiol.*, **10**, 125–133.
47. Yun,C.Y. and Fu,X.D. (2000) Conserved SR protein kinase functions in nuclear import and its action is counteracted by arginine methylation in Saccharomyces cerevisiae. *J. Cell. Biol.*, **150**, 707–718.
48. Raabe,C.A., Sanchez,C.P., Randau,G., Robeck,T., Skryabin,B.V., Chinni,S.V., Kube,M., Reinhardt,R., Ng,G.H., Manickam,R. *et al.* (2010) A global view of the nonprotein-coding transcriptome in Plasmodium falciparum. *Nucleic Acids Res.*, **38**, 608–617.
49. Epp,C., Li,F., Howitt,C.A., Chookajorn,T. and Deitsch,K.W. (2009) Chromatin associated sense and antisense noncoding RNAs are transcribed from the var gene family of virulence genes of the malaria parasite Plasmodium falciparum. *RNA*, **15**, 116–127.